
1 **Fire-climate interactions through aerosol radiative effect in a global chemistry-climate-**
2 **vegetation model**

3 Chenguang Tian^{1, 2}, Xu Yue¹, Jun Zhu¹, Hong Liao¹, Yang Yang¹, Yadong Lei³, Xinyi Zhou¹, Hao
4 Zhou², Yimain Ma², Yang Cao²

5 ¹ Jiangsu Key Laboratory of Atmospheric Environment Monitoring and Pollution Control,
6 Collaborative Innovation Center of Atmospheric Environment and Equipment Technology, School
7 of Environmental Science and Engineering, Nanjing University of Information Science &
8 Technology (NUIST), Nanjing, 210044, China

9 ² Climate Change Research Center, Institute of Atmospheric Physics, Chinese Academy of Sciences,
10 Beijing, 100029, China

11 ³ State Key Laboratory of Severe Weather & Key Laboratory of Atmospheric Chemistry of CMA,
12 Chinese Academy of Meteorological Sciences, Beijing, 100081, China

13
14 **Corresponding author:** Xu Yue (Email: yuexu@nuist.edu.cn)
15

Formatted: Centered

16 **Abstract**

17 Fire emissions influence radiation, climate, and ecosystems through aerosol radiative effects.
18 Meanwhile, these instantaneous environmental perturbations can feed back to affect fire emissions.
19 However, the magnitude of such fire-climate interactionsfeedback remains unclear on the global
20 scale. Here, we quantify the impacts of fire aerosols on climate through direct, indirect, and albedo
21 effects based on the two-way simulations using a well-established chemistry-climate-vegetation
22 model. Globally, fire emissions cause a reduction of $-0.57 \text{ W} \pm 0.166 \text{ W m}^{-2}$ in net radiation at
23 the top of the atmosphere with dominant contributions by aerosol indirect effect (AIE).
24 Consequently, terrestrial surface air temperature decreases by $0.061 \pm 0.165 \text{ }^{\circ}\text{C}$ with coolings
25 of $>0.25^{\circ}\text{C}$ over eastern Amazon, western U.S., and boreal Asia. Both aerosol direct effect (ADE)
26 and AIE contribute to such cooling while the aerosol albedo effect (AAE) exerts an offset warming,
27 especially at high latitudes. Land precipitation decreases by $0.180 \pm 0.966 \text{ mm month}^{-1}$ (1.78 ±
28 9.56%) mainly due to the inhibition in central Africa by AIE. Such rainfall deficit further reduces
29 regional leaf area index (LAI) and lightning ignitions, leading to changes in fire emissions. Globally,
30 fire emissions reduce by 2%-3% because of the fire-induced changesfast responses in humidity,
31 lightning, and LAI. The fire-climate interactionsaerosol radiative effects may cause larger
32 perturbations to climate systems with likely more fires under global warming.

33

34 **Short summary**

35 We quantify the impacts of fire aerosols on climate through direct, indirect, and albedo effects.
36 We find global fire aerosols cause a-cooling of surface air temperature and an inhibition of
37 precipitation. These climatic perturbations further reduce regional leaf area index and lightning
38 ignitions, both of which are not beneficial for fire emissions. By considering the feedback of fire
39 aerosols on humidity, lightning, and LAIleaf area index, we predict a slight reduction in fire
40 emissions.

41

42 **Keywords:** Fire emissions; fire-climate interaction; radiative effect; climate feedback; ModelE2-
43 YIBs model

44

Formatted: Font: Not Bold

Formatted: Indent: First line: 0.74 cm, No widow/orphan control

45 **1 Introduction**

46 Fire occurs all year round in both hemispheres, burning about 1% of the Earth's surface and
47 emitting roughly 2–3 Pg (=10¹⁵ g) carbon into atmosphere every year (~~Van Der Werf et al.,~~
48 ~~2017~~)(~~van der Werf et al., 2017~~). Fire activities are strongly influenced by fuel availability,
49 ignition/suppression, and climate conditions (~~Flannigan et al., 2009~~)(~~Flannigan et al., 2009~~). The
50 fuel type, continuity, and amount affect fire occurrence and spread probability (~~Flannigan et al.,~~
51 ~~2013~~)(~~Flannigan et al., 2013~~). Lightning discharge is the most important natural source of fire
52 ignition (Macias Fauria and Johnson, 2006). Human activities affect fire patterns by adding ignition
53 sources or by suppressing processes (~~Andela et al., 2017~~)(~~Andela et al., 2017~~). Compared to the
54 above factors, climate shows a more dominant role in modulating fire activities through the changes
55 of fuel moisture and spread conditions (Flannigan and Harrington, 1988).

56 Fire exerts prominent impacts on Earth systems and human society through various processes.
57 Biomass burning emits a large amount of trace gases and aerosol particles into the troposphere,
58 affecting air quality at the local and downwind regions (Yue and Unger, 2018). *In situ* observations
59 showed that about one-third of the background particles in the free troposphere of North America
60 were originated from biomass burning (~~Hudson et al., 2004~~)(~~Hudson et al., 2004~~). Extremely intense
61 fires can even inject aerosols into stratosphere, where the particles were transported globally (~~Yu et~~
62 ~~al., 2019~~)(~~Yu et al., 2019~~). Fire-induced air pollution can reduce global terrestrial productivity of
63 unburned forests (Yue and Unger, 2018), leading to weakened carbon uptake by ecosystems. The
64 global transport of fire air pollution also causes large threats to public health by increasing the risks
65 of diseases and mortality (~~Liu et al., 2015~~)(~~Liu et al., 2015~~). It is estimated that fire-induced
66 particulate matter causes more than 33,000 deaths globally each year (Chen *et al.*, 2021).

Formatted: Font: Italic

67 Aerosols from fires can cause substantial ~~feedbacks to impact on~~ climate ~~via radiative effect~~
68 owing to their different optical and chemical properties (~~Xu et al., 2021~~)(~~Xu et al., 2021~~). ~~Aerosol~~
69 ~~radiative effect is the instantaneous radiative impact on energy balance of climate system,~~
70 ~~representing the fast adjustment or response before changing global mean surface air temperature~~
71 ~~(TAS)~~. First, aerosols scatter and/or absorb solar radiation through aerosol direct effect (ADE),
72 leading to altered energy budget and climate variables (~~Carslaw et al., 2010~~)(~~Carslaw et al., 2010~~).
73 There is no agreement on the sign of ADE of biomass burning aerosols at the global scale. Some
74 studies (Heald *et al.*, 2014; Veira *et al.*, 2015; Zou *et al.*, 2020) predicted positive forcing while

Formatted: Font: Italic

Formatted: Font: Italic

Formatted: Font: Italic

75 others (Ward *et al.*, 2012; Jiang *et al.*, 2016; Grandey *et al.*, 2016) yielded negative forcing (−0.2 to
76 0.2 W m^{−2}), mainly because of the large uncertainties in the absorption of fire-emitted black carbon
77 (BC) (Carslaw *et al.*, 2010; Ipee, 2014)(Carslaw *et al.*, 2010; IPCC, 2014). Second, aerosols can
78 serve as cloud condensation nuclei (CCN) or ice nuclei to affect the microphysical properties of
79 cloud. Such aerosol indirect effect (AIE) further influences climate system through the changes of
80 cloud albedo and lifetime (Twomey, 1974; Albrecht, 1989). Globally, fire aerosols account for ~30%
81 of the total CCN (Andreae *et al.*, 2004)(Andreae *et al.*, 2004) and the overall negative AIE of fire
82 aerosol is stronger than the ADE in magnitude (Liu *et al.*, 2014; Ward *et al.*, 2012; Jiang *et al.*, 2016).
83 Third, deposition of fire-emitted BC aerosols reduces surface albedo and promotes ice/snow melting,
84 which is called aerosol–albedo effect (AAE) (Hansen and Nazarenko, 2004; Warren and Wiscombe,
85 1980). Compared with other two effects, the AAE shows more regional characteristics (Kang *et al.*,
86 2020)(Kang *et al.*, 2020). These fire-induced disturbance in radiative fluxes further alter
87 meteorological and hydrologic variables, which in turn affect fire activities through the changes in
88 fuel moisture and weather conditions.

Formatted: Font: Italic

Formatted: Font: Italic

Formatted: Font: Italic

Formatted: Font: Italic

Formatted: Font: Italic

Formatted: Font: Italic

89 ~~The two-way interactions between fire and climate~~Impact of fire-induced instantaneous
90 climatic perturbations to fire activities on the global scale have not been fully assessed. While
91 observations revealed fire-induced perturbations to regional climate (Bali *et al.*, 2017; Zhuravleva
92 *et al.*, 2017), its feedback to fire activities are difficult to be isolated from the influences of
93 background climate. Models provide unique tools to explore fire-climate interactions resulting from
94 aerosol radiative effect especially at the regional to global scales. However, fire-climate
95 interactionsthey are not routinely included in most of Earth system models. The IPCC sixth
96 assessment report (AR6) did not provide a quantitative assessment of fire-climatesuch feedback as
97 well (Ipee, 2021). In this study, we explore the impacts of fire aerosols(IPCC, 2021). In this study,
98 we explore the impacts of fire aerosol radiative effect on climate and the consequent feedbacks to
99 fire emissions by using a well-established fire parameterization coupled to a chemistry-climate-
100 vegetation model ModelE2-YIBs (Yue and Unger, 2015). The main objectives are (1) to isolate the
101 radiative effects of fire aerosols through ADE, AIE, and AAE processes and (2) to quantify the
102 feedback of fire-induced instantaneous climate effects to fire emissions ~~and air pollutants~~.

Formatted: Font: Italic

Formatted: Font: Italic

103

104 2 Data and methods

105 **2.1 Data**

106 We use the emissions of ~~BC and organic carbon (OC) aerosols~~ from Global Fire Emission
107 Database version 4.1s (GFED4.1s) to validate the simulated fire emissions. The GFED4.1s provides
108 monthly fire emission fluxes of various air pollutants based on satellite retrieval of area burned from
109 the Moderate Resolution Imaging Spectroradiometer (MODIS) (~~Van Der Werf et al., 2017~~)(~~van~~
110 ~~der Werf et al., 2017~~). Area burned in GFED4.1s is mainly derived from the MODIS burned area
111 product (~~Giglio et al., 2013~~)(~~Giglio et al., 2013~~), taking into account "small" fires outside the burned
112 area maps based on active fire detections (~~Randerson et al., 2012~~)(~~Randerson et al., 2012~~). The
113 gridded fire emission dataset has a spatial resolution of 0.25°×0.25° and is available for every month
114 from July 1997. To ~~estimate~~~~compute~~ anthropogenic ignition and suppression effects, (see section
115 ~~2.3~~), we use a downscaled population density dataset from Gao (2017, 2020). Monthly sea surface
116 temperature (SST) and sea ice ~~concentration~~ (SIC) obtained from Hadley Centre Sea Ice and Sea
117 Surface Temperature (HadISST) dataset (~~Rayner et al., 2003~~)(~~Rayner et al., 2003~~) are used as the
118 boundary conditions for the climate model.

119

120 **2.2 ModelE2-YIBs model**

121 The chemistry-climate-vegetation model ModelE2-YIBs is used to simulate the two-way
122 coupling between fire aerosols and climate systems. The ModelE2-YIBs is composed of the NASA
123 Goddard Institute for Space Studies (GISS) ModelE2 model (Schmidt *et al.*, 2014) and the Yale
124 Interactive terrestrial Biosphere Model (YIBs) (Yue and Unger, 2015). The GISS ModelE2 is a
125 global climate-chemistry model with a horizontal resolution of 2° × 2.5° latitude by longitude and
126 40 vertical layers extending to the stratosphere (0.1hPa). ~~The model simulates gas-phase chemistry,~~
127 ~~aerosols, and interactions among them. Well-established schemes are used to calculate direct (Koeh~~
128 ~~et al., 2006), indirect (Menon et al., 2008; Menon et al., 2010), and albedo (Warren and Wiscombe,~~
129 ~~1980, 1985) effects of aerosol species on the climate. The dynamics and physics codes are executed~~
130 ~~every 30 minutes and the radiation code is calculated every 2.5 hours. It has been extensively~~
131 ~~evaluated for meteorological and chemical variables against observations, reanalysis products and~~
132 ~~other models, and widely used for studies of climate systems, atmospheric components, and their~~
133 ~~interactions (Schmidt et al., 2014).~~

134 The gas-phase chemistry scheme considers 156 chemical reactions among 51 species,

Formatted: Font: Italic

Formatted: Font: Italic

Formatted

135 including NO_x-HO_x-O_x-CO-CH₄ chemistry and different species of volatile organic compounds.
136 Aerosol species in ModelE2 include sulfate, nitrate, sea salt, dust, BC, and organic carbon (OC),
137 which are interactively calculated and tracked for both mass and number concentrations. The aerosol
138 microphysical scheme is based on the quadrature method of moments, which incorporates
139 nucleation, gas-particle mass transfer, new particle formation, particle emissions, aerosol phase
140 chemistry, condensational growth, and coagulation (Bauer *et al.*, 2008). The residence time of
141 aerosol species varies greatly in space and time due to different removal rates. Turbulent dry
142 deposition is determined by resistance-in-series scheme, which is closely coupled to the boundary
143 layer scheme and implemented between the surface layer (10 m) and the ground (Koch *et al.*, 2006).
144 The wet deposition consists of several processes including scavenging within and below cloud,
145 evaporation of falling rainout, transportation along convective plumes, and detrainment and
146 evaporation from convective plumes (Koch *et al.*, 2006; Shindell *et al.*, 2006).

147 In ModelE2, gases can be converted to aerosols through chemical reactions, while aerosols
148 affect photolysis and provide reaction surface for gases. For example, the formation of sulfate
149 aerosols is driven by modeled oxidants (Bell *et al.*, 2005), and the chemical production of nitrate
150 aerosols is dependent on nitric acid and gaseous ammonia (Bauer *et al.*, 2007). Moreover, the
151 disturbances of aerosols on climate systems via direct, indirect, and albedo effects are considered in
152 ModelE2. Size-dependent optical parameters of aerosols are calculated by the Mie scattering theory.
153 The first AIE is estimated by the prognostic treatment of cloud droplet number concentration, which
154 is a function of contact nucleation, auto-conversion, and immersion freezing (Menon *et al.*, 2008;
155 Menon *et al.*, 2010). The AAE of BC is considered by estimating the decline of surface albedo as a
156 function of aerosol concentrations at the top layer of snow or ice (Koch and Hansen, 2005). BC
157 content in snow is determined by measurement-based average scavenging ratios (Hansen and
158 Nazarenko, 2004). More detailed descriptions of ModelE2 can be found in Schmidt *et al.* (2014). It
159 has been extensively evaluated for meteorological and chemical variables against observations,
160 reanalysis products and other models, and widely used for studies of climate systems, atmospheric
161 components, and their interactions (Schmidt *et al.*, 2014).

162 YIBs is a process-based vegetation model that dynamically simulates tree growth and
163 terrestrial carbon fluxes with prescribed fractions of nine plant functional types (PFTs), including
164 deciduous broadleaf forest, evergreen needleleaf forest, evergreen broadleaf forest, tundra,

Formatted: Font: Italic

165 shrubland, C₃/C₄ grassland, and C₃/C₄ cropland. Essential biological processes such as
 166 photosynthesis, phenology, autotrophic and heterotrophic respiration are considered and
 167 parameterized using the state-of-the-art schemes (Yue and Unger, 2015). *Dynamic daily leaf area*
 168 *index (LAI) is estimated based on carbon allocation and prognostic phenology which is dependent*
 169 *on temperature and drought conditions.* Simulated tree height, phenology, *gross primary*
 170 *productivity and leaf area index (LAI)* agree well with site-level observations and/or satellite
 171 retrievals (Yue and Unger, 2015). The YIBs model joined the dynamic global vegetation model
 172 inter-comparison project TRENDY and showed reasonable performance of carbon fluxes against
 173 available observations (Friedlingstein, *et al.*, 2020). *In the coupled model, ModelE2 provides*
 174 *meteorological drivers to YIBs, which feeds back to alter land surface water and energy fluxes*
 175 *through changes in stomatal conductance, surface albedo, and LAI.* By incorporating YIBs into
 176 ModelE2, the new coupled model ModelE2-YIBs can simulate interactions between terrestrial
 177 ecosystems and climate systems through the exchange of water and energy fluxes, and chemical
 178 components (Yue and Unger, 2015; Yue *et al.*, 2017).

Formatted: Font: Italic

Formatted: Font: Italic

180 2.3 Fire parameterization

181 We implemented the active global fire parameterization from *Pechony and Shindell*
 182 *(2009)* Pechony and Shindell (2009) into ModelE2-YIBs model. The parameterization considers key
 183 fire-related processes including fuel flammability, lightning and human ignitions, and human
 184 suppressions. Flammability is a unitless metric indicating conditions favorable for fire occurrence,
 185 and is calculated using vapor pressure deficit (VPD, hPa), precipitation (R, *mm day⁻¹*), and LAI
 186 (m² m⁻²) as follows:

$$187 \quad \text{Flam} = \text{VPD} \times \text{LAI} \times e^{-C_R \times R} \quad (1)$$

188 Here, LAI represents vegetation density and is dynamically calculated by YIBs model. C_R is a
 189 constant set to 2. VPD is a vital indicator of flammability conditions:

$$190 \quad \text{VPD} = e_s \times \left(1 - \frac{\text{RH}}{100}\right) \quad (2)$$

191 where e_s is the saturation vapor pressure and RH is surface relative humidity. e_s can be
 192 calculated by Goff-Gratch equation:

$$193 \quad e_s = e_{st} \times 10^Z \quad (3)$$

194 where e_{st} is 1013.246 hPa and

$$195 \quad Z = a \times \left(\frac{T_s}{T} - 1 \right) + b \times \log \frac{T_s}{T} + c \times \left(10^{d \left(1 - \frac{T_s}{T} \right)} - 1 \right) + f \times \left(10^{h \left(\frac{T_s}{T} - 1 \right)} - 1 \right) \quad (4)$$

196 Here, a, b, c, d, f and h are constants set to -7.90298, 5.02808, -1.3816 $\times 10^{-7}$, 11.344, 8.1328 $\times 10^{-3}$
197 and -3.49149, respectively. T_s is boiling point of water and equal to 373.16 K. [VPD and LAI in Eq. \(1\)](#)
198 [are calculated in half-hourly and daily time step, respectively, while 30-day running average precipitation is employed to avoid unrealistically huge flammability fluctuations.](#)

200 Natural and anthropogenic ~~ignitions determine~~[ignition determines](#) whether the fire can actually
201 occur. [If ignition is zero, the resulting fire emissions will be zero, regardless of flammability.](#) Natural
202 ignition source I_N depends on cloud-to-ground lightning (CoGL~~);~~[\) rate](#), which is simulated by
203 ModelE2 following the parameterization of Price and Rind (1994):

$$204 \quad I_N = \text{CoGL} = \begin{cases} 3.44 \times 10^{-5} \times H^{4.9} & \text{over land} \\ 6.4 \times 10^{-4} \times H^{1.73} & \text{over ocean} \end{cases} \quad (5)$$

205 where H is the cloud depth (unit: km). ~~The number of anthropogenic ignition source I_A is~~
206 ~~calculated as follows:~~

207 [Humans influence fire activity by adding ignition sources and suppressing fire events, the rates](#)
208 [of which increase with population and to some extent counteract each other. The number of](#)
209 [anthropogenic ignition source \$I_A\$ \(number \$\text{km}^{-2} \text{month}^{-1}\$ \) is calculated as follows \(Venevsky *et al.*,](#)
210 [2002\):](#)

$$211 \quad I_A = k(\text{PD}) \times \text{PD} \times \alpha \quad (6)$$

212 where PD is population density (number/ ~~km^2~~ ; km^{-2}). $k(\text{PD}) = 6.8 \times \text{PD}^{-0.6}$ stands for ignition
213 potentials of human activity, ~~and assuming that people in scarcely populated areas interact more with~~
214 [the natural ecosystems and therefore produce more ignition potential.](#) α is ~~equal~~[the number of](#)
215 [potential ignitions per person per month and set to 0.03. Human activities can also suppress](#)

216 [In principle, the successful suppression of fires, especially is dependent on early detection. It](#)
217 [is reasonably assumed that fires are detected earlier and suppressed more effectively in highly](#)
218 [populated area. The areas. Therefore, the](#) fraction of non-suppressed fires F_{NS} can be expressed as:

$$219 \quad F_{NS} = c_1 + c_2 \times \exp(-\omega \times \text{PD}) \quad (7)$$

220 where c_1 , c_2 and ω are constants and set to 0.05, 0.95 and 0.05, respectively. [The selection of](#)
221 [constant values in Eq. \(7\) is done in a heuristic way, due to lack of quantified data globally. It](#)
222 [assumes that up to 95% of fires is suppressed in the densely populated regions but only 5% in](#)

Formatted: Indent: First line: 0.74 cm

223 [unpopulated areas.](#)

224 With the calculation of flammability (Flam), ignition (I_N and I_A), and non-suppression (F_{NS}),
225 the fire count density N_{fire} (unit: number $\text{km}^{-2} \text{km}^{-2}$) at a specific time step can be derived as:

$$226 \quad N_{\text{fire}} = \text{Flam} \times (I_N + I_A) \times F_{NS} \quad (8)$$

227 Finally, fire emissions of trace gases and particulate matters (FireEmis) are calculated as:

$$228 \quad \text{FireEmis} = N_{\text{fire}} \times \text{EF} \quad (9)$$

229 Here, EF is the PFT-specific emission factor of an air pollutant such as ~~black carbon (BC)~~, ~~organic~~
230 ~~carbon~~ (OC), NO_x , NH_3 , SO_2 , CO , CH_4 , Alkenes and Paraffin. For each ~~pollutant~~ species,
231 simulated gridded emissions are grouped by dominant PFT and compared to [GFED annual total](#)
232 emissions [from GFED4.1s](#) over the same grids. The EF is then calibrated to minimize the root-
233 mean-square error between the simulated and GFED data. [for all land grids](#). Such calibration adjusts
234 only the global total amount of fire emissions without changing the spatiotemporal pattern predicted
235 by the parameterization.

236 [Compared to fire indexes, such as Canadian Fire Weather Index system \(Wagner, 1987\), this](#)
237 [fire parameterization shows advantages in integrating the effects of meteorology, vegetation, natural](#)
238 [ignition, and human activities \(both ignition and suppression\) on fires. Furthermore, it is physically](#)
239 [straightforward and has been validated based on global observations \(Pechony and Shindell, 2009\).](#)
240 [In ModelE2-YIBs, fire emissions are affected by environmental factors following above](#)
241 [parameterizations. In turn, the radiative effects of fire-emitted aerosols feed back to affect those](#)
242 [climatic and ecological factors. We consider only the fire emissions at surface due to the large](#)
243 [uncertainties in depicting fire plume height \(Sofiev *et al.*, 2012; Ke *et al.*, 2021\). The fire emissions](#)
244 [include both primary aerosols and trace gases, the latter of which react with other species to form](#)
245 [the secondary aerosols. These particles could be transported across the globe by the three-](#)
246 [dimensional atmospheric circulation and eventually removed through either dry or wet deposition.](#)

247

248 **2.4 Simulations**

249 We perform four groups of sensitivity experiments (Table 1) with the ModelE2-YIBs model to
250 quantify the fire-climate interactions through different radiative processes. The first group with
251 suffix 'AD' considers only the ADE. The second (third) group with suffix 'AD_AI' ('AD_AA')
252 considers both ADE and AIE (ADE and AAE). The fourth group with suffix 'AD_AI_AA' includes

Formatted: Subscript

253 all three aerosol radiative effects (ADE, AIE, and AAE). Within each group, two runs are performed
254 with (YF) or without (NF) fire emissions. For YF simulations, fire-induced aerosols including
255 primarily emitted and secondarily formed are dynamically calculated based on fire
256 emissionsparameterization (see section 2.3) and atmospheric transport. These fire aerosolsemissions
257 cause radiative perturbations and the consequent changes in climatic variables, which feedback to
258 influence fire emissions. For NF simulations, fire emissions at each step are set to zero, are calculated
259 offline at each step without perturbing the climate system, which can be considered that there is no
260 fire emission. By comparing the climatic variables from the YF and NF runs in the first group, we
261 isolate the impacts of fire aerosols on climate through ADE. By comparing the climatic effects from
262 the first and second (third) groups, we isolate the AIE (AAE) of fire aerosols. By comparing the
263 climatic variables from YF and NF runs in the fourth group, the overall effect (ADE+AIE+AAE) is
264 obtained. Besides, the differences of fire emissions between simulations of “YF_AD_AI_AA” and
265 “NF_AD_AI_AA” represent the feedback of fire aerosol-induced environmental perturbations.

266 For each simulation, climatological mean CO₂ concentrations, SST/SIC, and population
267 density in the year 2000 during 1995-2005 are used as boundary conditions to drive the model. Such
268 configuration ignores the year-to-year variability in climate systems, which may cause significant
269 changes in annual fire emissions (Burton *et al.*, 2020). Each simulation is integrated for 25 years
270 with the first 5 years spinning up and the last 20 years-year averaged and analyzed. Student, Two-
271 tail student t-test is performed and to assess 90% confidence levels of the significant changes at
272 predicted radiative and climatic responses ($p < 0.1$ are analyzed). In this study, downward (upward)
273 radiative/heat fluxes are defined as positive (negative). Given that the model is driven by prescribed
274 SST and SIC, only the rapid adjustments of atmospheric variables are taken into account and we
275 mainly focus on climate changes over land grid. The radiative effect simulated with such model
276 configuration is termed the effective radiative forcing (ERF).

277

278 **3 Results**

279 **3.1 Model evaluation**

280 Simulated fire emissions of BC and OC show hotspots in the tropics, such as Amazon, Sahel,
281 central Africa, and Southeast Asia (Fig. S1). The large tropical fire emissions are related to abundant
282 vegetation and/or distinct dry seasons. Compared to GFED4.1s data, ModelE2-YIBs slightly

Formatted: Font: Not Italic

Formatted: Font: Times New Roman

283 underestimates boreal fire emissions especially over northern Asia and North America. On the
284 global scale, fire releases 1.85 ± 0.01 Tg ($1 \text{ Tg} = 10^{12} \text{ g}$) C year⁻¹ of BC and 16.8 ± 0.92 Tg C year
285 ⁻¹ of OC in ModelE2-YIBs, close to the 1.86 Tg C year⁻¹ of BC and 16.4 Tg C year⁻¹ of OC estimated
286 by GFED4.1s. In general, ModelE2-YIBs reasonably captures the spatial distribution of fire
287 emissions, with high spatial correlations of 0.67 ($p < 0.01$) for BC and 0.58 ($p < 0.01$) for OC, and
288 low normalized mean biases of 0.6% for BC and 2.4% for OC against satellite-based observations.

289

290 3.2 Fire-induced radiative perturbations

291 Fig. S2 shows the fire-induced changes in Aerosol Optical Depth (AOD) at 550nm. Fire
292 emissions largely enhance surface aerosols especially over tropical regions. Hotspots are located in
293 southern Africa and South America with regional enhancement larger than 0.05 . In addition, large
294 enhancement is also found at boreal high latitudes (> 0.01). At the global scale, fires enhance AOD
295 by 0.006 ± 0.001 with 0.010 ± 0.001 over land.

296 Fire aerosols cause large perturbations in net radiation at top of atmosphere (TOA). Globally,
297 the net radiation at TOA decreases 0.565 ± 0.166 W m⁻² by fire aerosols (Fig. 1a). Regionally,
298 negative changes are predicted over central Africa, western South America, western North America
299 and the boreal high latitudes. Diagnosis shows that fire-induced AIE dominates the reduction of
300 TOA flux with a global value of -0.44440 ± 0.264 W m⁻² (Fig. 1c), accounting for 78% of the total
301 ~~effects~~ TOA radiative effect by fire aerosols. The spatial correlation coefficient is 0.62 over land
302 grids between the perturbations by all aerosol effects and that by AIE alone. Compared to AIE, the
303 changes in TOA radiative fluxes are much smaller for fire ADE (-0.058 ± 0.213 W m⁻², Fig. 1b)
304 and AAE (-0.016 ± 0.283 W m⁻², Fig. 1d) with limited perturbations on land.

305 ~~At the surface, fire~~ Fire aerosols decrease net shortwave radiation ~~reaching the surface~~ up to 9
306 W m⁻² in central Africa and 7 W m⁻² in Amazon (Fig. 2a), where biomass burning emissions are
307 most intense (Fig. S1). Such pattern is in general consistent with the changes of TOA fluxes (Fig.
308 1a), leading to an average reduction of -1.23227 ± 0.216 W m⁻² in the shortwave radiation over
309 global land. The fire-induced ADE alone reduces land surface shortwave radiation by $0.65654 \pm$
310 0.353 W m⁻² with the maximum center in Amazon (Fig. S3a). As a comparison, the fire-induced
311 AIE causes a smaller reduction of -0.55553 ± 0.518 W m⁻² with the hotspot in central Africa (Fig.
312 S3c). The net effect of AAE (0.263 ± 0.551 W m⁻²) by fire aerosols is positive mainly because fire

313 AAE reduces surface albedo and increase shortwave radiation over Tibetan Plateau, ~~and~~ boreal high
314 latitudes, ~~and Australia~~ (Fig. S3e). However, the magnitude of AAE is much smaller compared to
315 that of ADE and AIE.

316 Changes in surface longwave radiation (Fig. 2b) are much smaller than those in shortwave
317 radiation (Fig. 2a). Regionally, positive changes are predicted in the western U.S., eastern Amazon,
318 and South Africa, where fire-induced surface cooling (Fig. 3a) decreases the upward longwave
319 radiation. On the global scale, fire aerosols cause a decrease of 0.28281 ± 0.371 W m⁻² in surface
320 upward longwave radiation. As a result, fire aerosols induce a net atmospheric absorption of 0.191
321 ± 0.227 W m⁻² over land grids (Fig. 2c). The reductions in surface shortwave radiation are largely
322 balanced by changes in heat fluxes at the surface, which shows an average decrease of $0.83826 \pm$
323 0.311 W m⁻² in the upward fluxes over land grids (Fig. ~~2e~~2d). Fire ADE and AIE lead to reductions
324 of 0.59503 ± 0.289 W m⁻² and 0.43432 ± 0.411 W m⁻² in surface upward heat fluxes, respectively
325 (Fig. S3b and S3d). Changes in sensible heat account for 82.2 % of the changes in total heat
326 reduction, much higher than the contributions of 17.8% by latent heat fluxes (Fig. S4). Regionally,
327 the upward sensible heat decreases in the western U.S. and Amazon mainly due to fire ADE, while
328 the upward latent heat decreases in central Africa mainly by fire AIE (Fig. S5).

329

330 3.3 Fire-induced fast climatic changes responses

Formatted: Font: Bold

331 In response to the perturbations in radiative fluxes, land ~~surface air temperature~~ (TAS)
332 decreases 0.061 ± 0.165 °C globally by fire aerosols (Fig. 3a). Such cooling is mainly located in
333 western U.S., Amazon, and boreal Asia, following the large reductions in shortwave radiation (Fig.
334 2a). Meanwhile, moderate warming is predicted at the high latitudes of both hemispheres especially
335 over the areas covered with land ice such as Greenland and Antarctica. Sensitivity experiments show
336 that both ADE (Fig. 4a) and AIE (Fig. 4c) of fire aerosols result in net cooling globally, with regional
337 reductions of TAS over boreal Asia and North America. In contrast, the fire AAE causes increases
338 of TAS over boreal Asia and North America (Fig. 4e), where the deposition of BC aerosols reduces
339 surface albedo. Consequently, the fire AAE results in a global warming of 0.054 ± 0.163 °C, which
340 in part offsets the cooling effects by the ADE and AIE of fire aerosols.

341 Meanwhile, global land precipitation decreases by 0.48180 ± 0.966 mm/month ($1.78 \pm 9.56\%$)
342 with great spatial heterogeneity (Fig. 3b). Decreased precipitation is predicted over central Africa,

343 boreal North America, and eastern Siberia. In contrast, increased rainfall is predicted in western
344 U.S., eastern Amazon, and northern Asia. The reduction of precipitation is mainly contributed by
345 fire AIE, which reduces cloud droplet size and inhibits local rainfall in central Africa (Fig. 4d).
346 Consequently, latent heat fluxes are reduced to compensate the rainfall deficit in central Africa (Fig.
347 S4b).

348

349 **3.4 Fire-climate interactions**

350 **3.4 Climate feedback to fire aerosol radiative effect**

351 The fire-aerosol-induced [changesfast response](#) in precipitation, VPD, lightning, and LAI can
352 feed back to affect fire emissions. However, these changes may have contrasting impacts on fire
353 activities. For example, the aerosol-induced reduction of precipitation in central Africa (Fig. 3b)
354 increases local VPD (Fig. 5a) and consequently causes more fire emissions. Meanwhile, such
355 enhanced drought condition inhibits plant growth and decreases local LAI (Fig. 5c), which has
356 negative impacts on fire emissions by reducing fuel density. Furthermore, the fire AIE inhibits the
357 development of convective cloud, which limits cloud height and the number of cloud-to-ground
358 lightning in central Africa (Fig. 5b), leading to reduced ignition sources and fire emissions.

359 To illustrate the joint the impacts of fire-aerosol-induced [instantaneous](#) climatic change, we
360 count the number out of the four factors contributing positive effects to fire emissions over land
361 grids (Fig. 5d). The larger (smaller) number indicates higher possibility of increasing (decreasing)
362 fire emissions. Most of areas show neutral number of 2, indicating offsetting effects of the changes
363 in fire-prone factors. Only 13.5 % of land grids show numbers higher than 2 with sparse distribution.
364 In contrast, 32.1 % of land grids show numbers smaller than 2, especially for the grids over Siberia
365 and western U.S. where the increased rainfall (Fig. 3b) and decreased VPD (Fig. 5a) inhibit fire
366 emissions. Furthermore, the regional reductions in lightning ignition or LAI promote the inhibition
367 effects. As a result, fire emissions in YF_AD_AI_AA [slightly](#) decrease by 31.0 ± 35.9 Gg year⁻¹
368 (1.7%) for BC and 493.6 ± 566.8 Gg year⁻¹ (2.9%) for OC compared to NF_AD_AI_AA in which
369 fire emissions do not perturb climate (Fig. 6).

370

371 **4 Conclusions and discussion**

372 We used the chemistry-climate-vegetation coupled model ModelE2-YIBs to quantify fire-

373 climate interactions through ADE, AIE, and AAE. Globally, fire aerosols decrease TOA net radiation
374 by 0.565 ± 0.166 W m⁻², dominated by the AIE over central Africa. Surface net solar radiation also
375 exhibits widespread reductions especially over fire-prone areas with compensations from the
376 decreased sensible and latent heat fluxes. Following the changes in radiation, ~~surface air~~
377 ~~temperature~~land TAS decreases by 0.061 ± 0.165 °C and ~~land~~precipitation decreases by $0.180 \pm$
378 0.966 mm/month, albeit with regional inconsistencies. The surface cooling is dominated by fire
379 ADE and AIE, while the drought tendency is mainly contributed by fire AIE with hotspots in central
380 Africa. AAE also plays an important role by introducing warming tendency at the mid-to-high
381 latitudes. ~~The~~These fire-induced ~~fast~~ climatic ~~changes~~responses further affect VPD, LAI, and
382 lightning ignitions, leading to reductions in global fire emissions of BC by 2% and OC by 3%.

383 Our predicted reduction of 0.565 ± 0.166 W m⁻² in TOA radiation by fire aerosols is close to
384 the estimate of -0.51 W m⁻² reported by ~~Jiang et al. (2016)~~Jiang *et al.* (2016) and -0.59 W m⁻² of
385 ~~Zou et al. (2020)~~Zou *et al.* (2020) using different models with prescribed SST/SIC and fire-induced
386 ADE, AIE and AAE (Table 2). Within such change, fire ADE alone makes a moderate contribution
387 of -0.96016 ± 0.283 W m⁻², falling within the range of -0.2 to 0.2 W m⁻² from other studies. The
388 large uncertainty of fire ADE is likely related to the discrepancies in the BC absorption among
389 climate models, which cause varied net effects when offsetting the radiative perturbations of
390 scattering aerosols. As a comparison, fire AIE in our model induces a significant radiative effect of
391 -0.44440 ± 0.264 W m⁻². However, such magnitude is much smaller than previous estimates of -0.7
392 to -1.1 W m⁻² using different models (Table 2). We further estimated a limited fire AAE of -0.02016
393 ± 0.283 W m⁻², consistent with previous findings showing insignificant role of AAE by fire aerosols
394 (Ward *et al.*, 2012; Jiang *et al.*, 2016). Our estimates of reductions in TAS and precipitation also fall
395 within the range of previous studies (Table 2).

396 Our estimates are subject to some limitations and uncertainties. First, we considered only the
397 fast climatic responses of land surface with prescribed SST and SIC in the simulations. Although
398 most of fire-induced AOD changes are located on land (Fig. S2), ~~the air-ocean interactions may~~
399 ~~cause complex feedbacks to aerosol radiative effects (Jiang et al., 2020). Such feedback should be~~
400 ~~explored in the future studies with a coupled ocean model.~~S2), the air-sea interaction may cause
401 complex climatic responses to aerosol radiative effects. In a recent study, Jiang *et al.* (2020)
402 emphasized the role of slow feedback contributed by fire aerosols on global precipitation reduction

Formatted: Font: Italic

Formatted: Font: Italic

403 [by using a coupled model. Such air-sea interaction will modify the magnitude and/or spatial pattern](#)
404 [of fast climatic responses revealed in this study, and should be explored in the future studies with](#)
405 [coupled ocean models.](#) Second, the nonlinear effects of different radiative processes may influence
406 the attribution results. In this study, we isolate the effects of AIE and AAE by subtracting variables
407 between different groups following the approaches by Bauer and Menon (2012). However, the
408 additive perturbations from individual processes are not equal to the total perturbations with all
409 processes in one simulation. For example, the sum of three processes causes changes of TOA
410 radiation by -0.54513 ± 0.324 W m⁻² (Figs 1b-1d), surface temperature by -0.037 ± 0.160 °C (Figs
411 4a, 4c, 4e), and precipitation by -1.09090 ± 1.122 mm month⁻¹ (Figs 4b, 4d, 4f). These perturbations
412 are weaker than the net effects of -0.57565 ± 0.166 W m⁻² (Fig. 1a) in radiation and $-0.061 \pm$
413 0.165 °C in temperature (Fig. 3a), but much stronger than that of -0.18 ± 0.96 mm month⁻¹ in
414 precipitation (Fig. 3b) predicted by the simulation with all three processes. As a result, the nonlinear
415 feedbacks among different radiative processes may magnify or offset the final climatic responses to
416 fire aerosols. [Third, considering the complex nature of fire activities, the fire parameterization in](#)
417 [this study does not incorporate all fire-related processes \(e.g., the influence of wind\). In addition,](#)
418 [the simulations omit several factors influencing fire emissions \(e.g., moist content of fuels\) and](#)
419 [aerosol radiative effects \(e.g. fire plume height\). For example, studies show significant impacts of](#)
420 [plume rise on the vertical distribution of fire aerosols and the consequent radiative effects \(Walter](#)
421 [et al., 2016\). The impacts of human activity on fire emissions are calculated as a function of](#)
422 [population density without considerations of differences in economy, education, and policies. These](#)
423 [auxiliary factors may increase the spatial heterogeneity of fire aerosol radiative effects and deserve](#)
424 [further explorations in the future studies.](#)

425 Despite these limitations, we made the first attempt to assess the two-way interaction between
426 fire emissions and climate: [via aerosol radiative effects.](#) Our results show that fire-emitted aerosols
427 cause negative [effective radiative forcing \(ERF\)](#) of -0.57565 ± 0.166 W m⁻², which is about 20% of
428 the anthropogenic ERF due to the increased greenhouse gases and aerosols from 1950 to 2019 ~~(Fpee,~~
429 ~~2021)~~(IPCC, 2021). Such fire ERF largely reduces ~~surface air temperature and~~ regional TAS and
430 precipitation, leading to further changes in fire emissions. Although the reduction of -2% to -3% in
431 fire emissions by the fire-climate interaction [through aerosol radiative effect](#) seems limited, such
432 change is a result of several complex feedbacks that may exert offsetting effects. Furthermore, our

Formatted

Formatted

Formatted

Formatted

Formatted

433 simulations reveal a strong inhibition effect of fire aerosols on LAI in central Africa due to the
434 aerosol-induced drought intensification. Such negative effects on ecosystems are inconsistent with
435 previous estimates that showed certain fertilization effects by fire aerosols (Yue and Unger, 2018),
436 mainly because the rainfall deficit overweighs the diffuse fertilization effects of aerosols. With likely
437 more fires under global warming (~~Abatzoglou et al., 2019~~)(Abatzoglou *et al.*, 2019), our results
438 suggested complex and uncertain perturbations by fire emissions to ~~radiation,~~ climate, and
439 ecosystem through fire-climate interactions.

440

441 **Acknowledgements**

442 The authors are grateful to Dr. Matthew Kasoar and another anonymous reviewer for their
443 constructive comments that have improved this study.

444

445 **Financial support**

446 This research was supported by the National Key Research and Development Program of China
447 (grant no. 2019YFA0606802)._

448

449 **Competing Interests**

450 The authors declare that they have no conflict of interest.

451

452 **Data availability**

453 Hadley Centre Sea Ice and Sea Surface Temperature dataset were obtain from
454 <https://www.metoffice.gov.uk/hadobs/hadisst/>. Population data could be downloaded form
455 <https://cmr.earthdata.nasa.gov/search/concepts/C1739468823-SEDAC.html>. GFED data were
456 obtained from https://daac.ornl.gov/VEGETATION/guides/fire_emissions_v4_R1.html.

457

458 **Reference:**

459 Abatzoglou, J. T., Williams, A. P., and Barbero, R.: 2019 Global Emergence of Anthropogenic Climate
460 Change in Fire Weather Indices, *Geophysical Research Letters*, **46**, 326-336,
461 [10.1029/2018gl080059](https://doi.org/10.1029/2018gl080059), 2019,36

462 Albrecht, B. A.: 1989 Aerosols, Cloud Microphysics, and Fractional Cloudiness, **245**, 1227-1230,
463 [doi:10.1126/science.245.4923.1227](https://doi.org/10.1126/science.245.4923.1227), 1989,30

464 Andela, N., Morton, D. C., Giglio, L., Chen, Y., van der Werf, G. R., Kasibhatla, P. S., DeFries, R.
465 S., Collatz, G. J., Hantson, S., Kloster, S., Bachelet, D., Forrest, M., Lasslop, G., Li, F.,
466 Mangeon, S., Melton, J. R., Yue, C., and Randerson, J. T.: 2017 A human-driven decline in
467 global burned area, *Science*, **356**, 1356, [10.1126/science.aal4108](https://doi.org/10.1126/science.aal4108), 2017.

468 Andreae, M. O., Rosenfeld, D., Artaxo, P., Costa, A. A., Frank, G. P., Longo, K. M., and Silva-Dias,
469 M. A. F.: 2004 Smoking Rain Clouds over the Amazon, **303**, 1337-1342,
470 [doi:10.1126/science.1092779](https://doi.org/10.1126/science.1092779), 2004,42

471 Bali, K., Mishra, A. K., and Singh, S.: 2017 Impact of anomalous forest fire on aerosol radiative forcing
472 and snow cover over Himalayan region, *Atmospheric Environment*, **150**, 264-275,
473 <https://doi.org/10.1016/j.atmosenv.2016.11.061>, 2017,75

474 Bauer, S. E. and Menon, S.: 2012 Aerosol direct, indirect, semidirect, and surface albedo effects from
475 sector contributions based on the IPCC AR5 emissions for preindustrial and present-day
476 conditions, **117**, <https://doi.org/10.1029/2011JD016816>, 2012, **117**,

477 <https://doi.org/10.1029/2011JD016816>, 2012, **117**,
478 <https://doi.org/10.1029/2011JD016816>, 2012, **117**,
479 <https://doi.org/10.1029/2011JD016816>, 2012, **117**

480 [Bauer S E, Mishchenko M I, Lacis A A, Zhang S, Perlwitz J and Metzger S M 2007 Do sulfate and nitrate
481 coatings on mineral dust have important effects on radiative properties and climate modeling?
482 **112**](https://doi.org/10.1029/2011JD016816)

483 [Bauer S E, Wright D L, Koch D, Lewis E R, McGraw R, Chang L S, Schwartz S E and Ruedy R 2008
484 MATRIX \(Multiconfiguration Aerosol TRacker of mIXing state\): an aerosol microphysical
485 module for global atmospheric models *Atmos. Chem. Phys.* **8** 6003-35](https://doi.org/10.1029/2011JD016816)

486 [Bell N, Koch D and Shindell D T 2005 Impacts of chemistry-aerosol coupling on tropospheric ozone and
487 sulfate simulations in a general circulation model **110**](https://doi.org/10.1029/2011JD016816)

488 [Burton C, Betts R A, Jones C D, Feldpausch T R, Cardoso M and Anderson L O 2020 El Niño Driven
489 Changes in Global Fire 2015/16 **8**](https://doi.org/10.1029/2011JD016816)

490 Carslaw, K. S., Boucher, O., Spracklen, D. V., Mann, G. W., Rae, J. G., L., Woodward, S., and Kulmal,
491 M.: 2010 A review of natural aerosol interactions and feedbacks within the Earth system, *Atmos.
492 Chem. Phys.*, **10**, 1701-1737, [10.5194/acp-10-1701-2010](https://doi.org/10.5194/acp-10-1701-2010), 2010,37

493 Chen, G., Guo, Y., Yue, X., Tong, S., Gasparrini, A., Bell, M., L., Armstrong, B., Schwartz, J.,
494 Jaakkola, J., J., K., Zanobetti, A., Lavigne, E., Nascimento Saldiva, P., H., Kan, H., Royé,
495 D., Milojevic, A., Overcenco, A., Urban, A., Schneider, A., Entezari, A., Vicedo-Cabrera, A.,
496 M., Zeka, A., Tobias, A., Nunes, B., Alahmad, B., Forsberg, B., Pan, S., C., Íñiguez, C.,
497 Ameling, C., De la Cruz Valencia, C., Åström, C., Houthuijs, D., Van Dung, D., Samoli, E.,
498 Mayvaneh, F., Sera, F., Carrasco-Escobar, G., Lei, Y., Orru, H., Kim, H., Holobaca, I., H.,
499 Kyselý, J., Teixeira, J., P., Madureira, J., Katsouyanni, K., Hurtado-Díaz, M., Maasikmets,
500 M., Ragettli, M., S., Hashizume, M., Stafoggia, M., Pascal, M., Scortichini, M., de Sousa
501 Zanotti Stagliorio Coelho, M., Valdés Ortega, N., Rytíř, N., R., I., Scovronick, N., Matus, P.,
Goodman, P., Garland, R., M., Abrutzky, R., Garcia, S., O., Rao, S., Fratianni, S., Dang, T.,
N., Colistro, V., Huber, V., Lee, W., Seposo, X., Honda, Y., Guo, Y., L., Ye, T., Yu, W.,
Abramson, M., J., Samet, J., M., and Li, S.: 2021 Mortality risk attributable to wildfire-related

Formatted: Indent: Left: 0 cm, Hanging: 7.2 ch

Formatted: Font: Italic

Formatted: Font: Bold

Formatted: Font: Bold

Formatted: Font: Italic

Formatted: Font: Bold

Formatted: Font: Bold

Formatted: Font: Italic

Formatted: Font: Bold

Formatted: Font: Bold

Formatted: Indent: Left: 0 cm, Hanging: 7.2 ch

Formatted: Font: Italic

Formatted: Font: Bold

502 PM_{2.5} pollution: a global time series study in 749 locations; *The Lancet*
503 *Planetary Health*, **5**, e579–e587, [10.1016/S2542-5196\(21\)00200-X](https://doi.org/10.1016/S2542-5196(21)00200-X), 2021, e87

504 Flannigan, M. M., Cantin A. S., de Groot W. J., Wotton M., Newbery A. and Gowman L. M. 2013 Global
505 wildland fire season severity in the 21st century *Forest Ecology and Management* **294** 54–61

506 Flannigan M. and Harrington, J. B.: 1988 A Study of the Relation of Meteorological Variables to Monthly
507 Provincial Area Burned by Wildfire in Canada (1953–80), *Journal of Applied Meteorology and*
508 *Climatology*, **27**, 441–452, [10.1175/1520-0450\(1988\)027<0441:ASOTRO>2.0.CO;2](https://doi.org/10.1175/1520-0450(1988)027<0441:ASOTRO>2.0.CO;2), 1988, 52

509 Flannigan, M., Krawchuk, M. A., de Groot, W. J., Wotton, B. M., and Gowman, L. M.: 2009
510 Implications of changing climate for global wildland fire %J *International Journal of Wildland*
511 *Fire*, **18**, 483–507, <https://doi.org/10.1071/WFE08187>, 2009.

512 Flannigan, M., Cantin, A. S., de Groot, W. J., Wotton, M., Newbery, A., and Gowman, L. M.: Global
513 wildland fire season severity in the 21st century, *Forest Ecology and Management*, **294**, 54–61,
514 <https://doi.org/10.1016/j.foreco.2012.10.022>, 2013.

515 Friedlingstein, P., O'Sullivan, M., Jones, M. W., Andrew, R. M., Hauck, J., Olsen, A., Peters, G., Pongratz,
516 W., Pongratz, J., Sitch, S., Le Quéré, C., Canadell, J. G., Ciais, P., Jackson, R. B., Alin,
517 S., Aragão, L. E. O. C., Arneeth, A., Arora, V., Bates, N., Becker, M., Benoit-Cattin,
518 A., Bittig, H., Bopp, L., Bultan, S., Chandra, N., Chevallier, F., Chini, L., Evans, W.,
519 Florentie, L., Forster, P., Gasser, T., Gehlen, M., Gilfillan, D., Gkritzalis, T., Gregor, L.,
520 Gruber, N., Harris, I., Hartung, K., Haverd, V., Houghton, R. A., Ilyina, T., Jain, A., Kato,
521 Joetzier, E., Kadono, K., Kato, E., Kitidis, V., Korsbakken, J., Landschützer, P., Lefèvre,
522 N., Lenton, A., Lienert, S., Liu, Z., Lombardozzi, D., Marland, G., Metz, N., Munro, D.,
523 R., Nabel, J. E. M., Nakaoka, S., Niwa, Y., O'Brien, K., Ono, T., Palmer, P., Pierrot,
524 D., Poulter, B., Resplandy, L., Robertson, E., Rödenbeck, C., Schwinger, J., Séférian, R.,
525 Skjelvan, I., Smith, A. J., Sutton, A. J., Tanhua, T., Tans, P., Tian, H., Tilbrook, B., van
526 der Werf, G., Vuichard, N., Walker, A., Wanninkhof, R., Watson, A., Willis, D.,
527 Wiltshire, A. J., Yuan, W., Yue, X., and Zaehle, S.: 2020 Global Carbon Budget 2020, *Earth*
528 *Syst. Sci. Data*, **12**, 3269–3340, [10.5194/essd-12-3269-2020](https://doi.org/10.5194/essd-12-3269-2020), 2020, 340

529 Gao, J.: 2017 Downscaling Global Spatial Population Projections from 1/8-degree to 1-km Grid Cells,
530 2017.

531 Gao, J.: 2020 Global 1-km Downscaled Population Base Year and Projection Grids Based on the Shared
532 Socioeconomic Pathways, Revision 01, (Palisades, NY: NASA Socioeconomic Data and
533 Applications Center (SEDAC) [dataset], 2020.)

534 Giglio, L., Randerson, J. T., and van der Werf, G. R.: 2013 Analysis of daily, monthly, and annual burned
535 area using the fourth-generation global fire emissions database (GFED4), *Journal of*
536 *Geophysical Research: Biogeosciences*, **118**, 317–328, <https://doi.org/10.1002/jgrg.20042>,
537 2013, 28

538 Grandey, B., S., Lee, H., H., and Wang, C.: 2016 Radiative effects of interannually varying vs.
539 interannually invariant aerosol emissions from fires, *Atmos. Chem. Phys.*, **16**, 14495–14513,
540 [10.5194/acp-16-14495-2016](https://doi.org/10.5194/acp-16-14495-2016), 2016, 513

541 Hansen, J. and Nazarenko, L.: 2004 Soot climate forcing via snow and ice albedos, **101**, 423–428,
542 [10.1073/pnas.2237157100](https://doi.org/10.1073/pnas.2237157100) %J *Proceedings of the National Academy of Sciences of the United*
543 *States of America*, 2004, 8

544 Heald, C., L., Ridley, D., A., Kroll, J., H., Barrett, S., R., H., Cady-Pereira, K., E., Alvarado, M., J., and
545 Holmes, C., D.: 2014 Contrasting the direct radiative effect and direct radiative forcing of

Formatted: Font: Italic

Formatted: Font: Bold

Formatted: Indent: Left: 0 cm, Hanging: 7.2 ch

Formatted: Font: Italic

Formatted: Font: Bold

Formatted: Font: Bold

Formatted: Indent: Left: 0 cm, Hanging: 7.2 ch

Formatted: Font: Italic

Formatted: Font: Bold

Formatted: Font: Italic

Formatted: Font: Bold

Formatted: Font: Italic

Formatted: Font: Bold

Formatted: Font: Bold

546 aerosols; *Atmos. Chem. Phys.*, **14**, 5513–5527, [10.5194/acp-14-5513-2014](https://doi.org/10.5194/acp-14-5513-2014), 2014, 27

547 Hudson, P. K., Murphy, D. M., Cziczo, D. J., Thomson, D. S., de Gouw, J. A., Warneke, C., Holloway,

548 J., Jost, H.-J., and Hübner, G.: 2004 Biomass-burning particle measurements: Characteristic

549 composition and chemical processing, **109**, <https://doi.org/10.1029/2003JD004398>, 2004,

550 IPCC: 2014 *Contribution of Working Groups I, II and III to the Fifth Assessment Report of the*

551 *Intergovernmental Panel on Climate Change [Core Writing Team, R.K. Pachauri and L.A.*

552 *Meyer (eds.)]* (IPCC, Geneva, Switzerland, 151 pp, 2014).

553 IPCC: 2021 *Climate Change 2021: The Physical Science Basis. Contribution of Working Group I to the*

554 *Sixth Assessment Report of the Intergovernmental Panel on Climate Change [Masson-Delmotte,*

555 *V., P. Zhai, A. Pirani, S. L. Connors, C. Péan, S. Berger, N. Caud, Y. Chen, L. Goldfarb, M. I.*

556 *Gomis, M. Huang, K. Leitzell, E. Lonnoy, J. B. R. Matthews, T. K. Maycock, T. Waterfield, O.*

557 *Yelekçi, R. Yu and B. Zhou (eds.)]* vol In Press.: Cambridge University Press, 2021.)

558 Jiang, Y., Lu, Z., Liu, X., Qian, Y., Zhang, K., Wang, Y., and Yang, X. Q.: 2016 Impacts of global

559 open-fire aerosols on direct radiative, cloud and surface-albedo effects simulated with CAM5;

560 *Atmos. Chem. Phys.*, **16**, 14805–14824, [10.5194/acp-16-14805-2016](https://doi.org/10.5194/acp-16-14805-2016), 2016, 24

561 Jiang, Y., Yang, X.-Q., Liu, X., Qian, Y., Zhang, K., Wang, M., Li, F., Wang, Y., and Lu, Z.: 2020

562 Impacts of Wildfire Aerosols on Global Energy Budget and Climate: The Role of Climate

563 Feedbacks; *Journal of Climate*, **33**, 3351–3366, [10.1175/JCLI-D-19-0572.1](https://doi.org/10.1175/JCLI-D-19-0572.1), 2020, 66

564 Kang, S., Zhang, Y., Qian, Y., and Wang, H.: 2020 A review of black carbon in snow and ice and its

565 impact on the cryosphere; *Earth-Science Reviews*, **210**, 103346,

566 <https://doi.org/10.1016/j.earscirev.2020.103346>, 2020.

567 Ke Z., Wang Y., Zou Y., Song Y. and Liu Y. 2021 Global Wildfire Plume-Rise Data Set and

568 Parameterizations for Climate Model Applications **126** e2020JD033085

569 Koch, D and Hansen J 2005 Distant origins of Arctic black carbon: A Goddard Institute for Space Studies

570 ModelE experiment *Journal of Geophysical Research: Atmospheres* **110**

571 *Koch* D., Schmidt, G. A., and Field, C. V.: 2006 Sulfur, sea salt, and radionuclide aerosols in GISS

572 ModelE, **111**, <https://doi.org/10.1029/2004JD005550>, 2006,

573 Liu, J., C., Pereira, G., Uhl, S., A., Bravo, M., A., and Bell, M., L.: 2015 A systematic review of the

574 physical health impacts from non-occupational exposure to wildfire smoke; *Environmental*

575 *Research*, **136**: 120–132, <https://doi.org/10.1016/j.envres.2014.10.015>, 2015, 32

576 Liu, Y., Goodrick, S., and Heilman, W.: 2014 Wildland fire emissions, carbon, and climate: Wildfire–

577 climate interactions; *Forest Ecology and Management*, **317**, 80–96,

578 <https://doi.org/10.1016/j.foreco.2013.02.020>, 2014.

579 Macias Fauria, M. and Johnson, E. A.: 2006 Large-scale climatic patterns control large lightning fire

580 occurrence in Canada and Alaska forest regions; *Journal of Geophysical Research:*

581 *Biogeosciences*, **111**, <https://doi.org/10.1029/2006JG000181>, 2006,

582 Menon, S., Koch, D., Beig, G., Sahu, S., Fasullo, J., and Orlikowski, D.: Black carbon aerosols and the

583 third polar ice cap. *Atmos. Chem. Phys.*, **10**, 4559–4571, [10.5194/acp-10-4559-2010](https://doi.org/10.5194/acp-10-4559-2010), 2010.

584 Menon, S., Del Genio, A. D., Kaufman, Y., Bennartz, R., Koch, D., Loeb, N., and Orlikowski, D.:

585 2008 Analyzing signatures of aerosol-cloud interactions from satellite retrievals and the GISS

586 GCM to constrain the aerosol indirect effect. **113**, <https://doi.org/10.1029/2007JD009442>, 2008,

587 **113**,

588 Menon S, Koch D, Beig G, Sahu S, Fasullo J and Orlikowski D 2010 Black carbon aerosols and the third

589 polar ice cap *Atmos. Chem. Phys.* **10** 4559–71

Formatted: Font: Italic

Formatted: Font: Bold

Formatted: Font: Bold

Formatted: Font: Bold

Formatted: Font: Italic

Formatted: Font: Italic

Formatted: Font: Italic

Formatted: Font: Bold

Formatted: Font: Italic

Formatted: Font: Bold

Formatted: Font: Italic

Formatted: Font: Bold

Formatted: Indent: Left: 0 cm, Hanging: 7.2 ch

Formatted: Font: Bold

Formatted: Font: Bold

Formatted: Font: Italic

Formatted: Font: Bold

Formatted: Font: Italic

Formatted: Font: Bold

Formatted: Font: Italic

Formatted: Font: Bold

Formatted: Font: Bold

Formatted: Indent: Left: 0 cm, Hanging: 7.2 ch

Formatted: Font: Bold

590 Pechony, O. and Shindell, D. T.: 2009 Fire parameterization on a global scale, *Journal of Geophysical*
591 *Research*, **114**, <https://doi.org/10.1029/2009JD011927>, 2009.

592 Price, C. and Rind, D.: 1994 Modeling Global Lightning Distributions in a General Circulation Model,
593 *Monthly Weather Review*, **122**, 1930-1939, [10.1175/1520-0493\(1994\)122<1930:MGLDIA>2.0.CO;2](https://doi.org/10.1175/1520-0493(1994)122<1930:MGLDIA>2.0.CO;2), 1994-9

594 Randerson, J. T., Chen, Y., van der Werf, G. R., Rogers, B. M., and Morton, D. C.: 2012 Global burned
595 area and biomass burning emissions from small fires, *Journal of Geophysical Research:*
596 *Biogeosciences*, **117**, <https://doi.org/10.1029/2012JG002128>, 2012.

597 Rayner, N. A., Parker, D. E., Horton, E. B., Folland, C. K., Alexander, L. V., Rowell, D. P., Kent, E.
598 C., and Kaplan, A.: 2003 Global analyses of sea surface temperature, sea ice, and night marine
599 air temperature since the late nineteenth century, **108**, <https://doi.org/10.1029/2002JD002670>,
600 **2003**, **108**.

601 Schmidt, G. A., Kelley, M., Nazarenko, L., Ruedy, R., Russell, G. L., Aleinov, I., Bauer, M., Bauer,
602 S. E., Bhat, M. K., Bleck, R., Canuto, V., Chen, Y., H., Cheng, Y., Clune, T. L., Del Genio,
603 A., de Fainchtein, R., Faluvegi, G., Hansen, J. E., Healy, R. J., Kiang, N. Y., Koch, D., Lacis,
604 A. A., LeGrand, A. N., Lerner, J., Lo, K. K., Matthews, E. E., Menon, S., Miller, R. L.,
605 Oinas, V., Olos, A., Perlwitz, J. P., Puma, M. J., Putman, W. M., Rind, D., Romanou,
606 A., Sato, M., Shindell, D. T., Sun, S., Syed, R. A., Tausnev, N., Tsigaridis, K., Unger, N.,
607 Voulgarakis, A., Yao, M., S., and Zhang, J.: 2014 Configuration and assessment of the GISS
608 ModelE2 contributions to the CMIP5 archive, *Journal of Advances in Modeling Earth Systems*,
609 **6**, 141-184, [10.1002/2013MS000265](https://doi.org/10.1002/2013MS000265), 2014, 84

610 [Shindell D T, Faluvegi G, Unger N, Aguilar E, Schmidt G A, Koch D M, Bauer S E and Miller R L 2006](https://doi.org/10.1002/2013MS000265)
611 [Simulations of preindustrial, present-day, and 2100 conditions in the NASA GISS composition](https://doi.org/10.1002/2013MS000265)
612 [and climate model G-PUCCINI *Atmos. Chem. Phys.* **6** 4427-59](https://doi.org/10.1002/2013MS000265)

613 [Sofiev M, Ermakova T and Vankevich R 2012 Evaluation of the smoke-injection height from wild-land](https://doi.org/10.1002/2013MS000265)
614 [fires using remote-sensing data *Atmos. Chem. Phys.* **12** 1995-2006](https://doi.org/10.1002/2013MS000265)

615 Twomey, S.: 1974 Pollution and the planetary albedo, *Atmospheric Environment (1967)*, **8**, 1251-1256,
616 [https://doi.org/10.1016/0004-6981\(74\)90004-3](https://doi.org/10.1016/0004-6981(74)90004-3), 1974-6

617 van der Werf, G. R., Randerson, J. T., Giglio, L., van Leeuwen, T. T., Chen, Y., Rogers, B. M., Mu,
618 M., van Marle, M. J., Morton, D. C., Collatz, G. J., Yokelson, R. J., and Kasibhatla, P. S.:
619 2017 Global fire emissions estimates during 1997–2016, *Earth Syst. Sci. Data*, **9**, 697-720,
620 [10.5194/essd-9-697-2017](https://doi.org/10.5194/essd-9-697-2017), 2017.

621 Veira, A., Kloster, S., Schutgens, N.-A. J., and Kaiser, J. W.: 2015 Fire emission heights in the climate
622 system – Part 2: Impact on transport, black carbon concentrations and radiation, *Atmos. Chem.*
623 *Phys.*, **15**, 7173-7193, [10.5194/acp-15-7173-2015](https://doi.org/10.5194/acp-15-7173-2015), 2015-93

624 Venevsky, S., Thonicke, K., Sitch, S. and Cramer, W.: 2002 Simulating fire regimes in human-dominated
625 ecosystems: Iberian Peninsula case study *Global Change Biology* **8** 984-98

626 Wagner, V.: 1987 *Development and structure of the Canadian Forest Fire Weather Index System*, *Forestry*
627 *Technical Report*: Canadian Forestry Service)

628 Walter, C., Freitas, S. R., Kottmeier, C., Kraut, I., Rieger, D., Vogel, H. and Vogel, B.: 2016 The importance of
629 plume rise on the concentrations and atmospheric impacts of biomass burning aerosol *Atmos.*
630 *Chem. Phys.* **16** 9201-19

631 Ward, D., S., Kloster, S., Mahowald, N., M., Rogers, B. M., Randerson, J. T., and Hess, P. G.: 2012 The
632 changing radiative forcing of fires: global model estimates for past, present and future, *Atmos.*

Formatted: Indent: Left: 0 cm, Hanging: 7.2 ch

Formatted: Font: Italic

Formatted: Font: Bold

Formatted: Font: Bold

Formatted: Font: Italic

Formatted: Font: Bold

Formatted: Font: Italic

Formatted: Font: Bold

Formatted: Font: Bold

Formatted: Font: Bold

Formatted: Font: Bold

Formatted: Font: Italic

Formatted: Font: Bold

Formatted: Indent: Left: 0 cm, Hanging: 7.2 ch

Formatted: Font: Italic

Formatted: Font: Bold

Formatted: Font: Italic

Formatted: Font: Bold

Formatted: Indent: Left: 0 cm, Hanging: 7.2 ch

Formatted: Font: Italic

634 *Chem. Phys.*, **12**, 10857-10886, [10.5194/aep-12-10857-2012](https://doi.org/10.5194/aep-12-10857-2012), 2012, 86

635 Warren, S. G. and Wiscombe, W. J.: 1980 A Model for the Spectral Albedo of Snow. II: Snow Containing
 636 Atmospheric Aerosols %J *Journal of Atmospheric Sciences*, **37**, 2734-2745, [10.1175/1520-](https://doi.org/10.1175/1520-0469(1980)037<2734:Amfisa>2.0.Co;2)
 637 [0469\(1980\)037<2734:Amfisa>2.0.Co;2](https://doi.org/10.1175/1520-0469(1980)037<2734:Amfisa>2.0.Co;2), 1980, **37** 2734-45

638 Warren, S. G. and Wiscombe, W. J.: Dirty snow after nuclear war, *Nature*, **313**, 467-470,
 639 [10.1038/313467a0](https://doi.org/10.1038/313467a0), 1985.

640 Xu, L., Zhu, Q., Riley, W. J., Chen, Y., Wang, H., Ma, P., L., and Randerson, J. T.: 2021 The Influence
 641 of Fire Aerosols on Surface Climate and Gross Primary Production in the Energy Exascale Earth
 642 System Model (E3SM), *Journal of Climate*, **34**, 7219-7238, [10.1175/JCLI-D-21-0193.1](https://doi.org/10.1175/JCLI-D-21-0193.1),
 643 [2021-38](https://doi.org/10.1175/JCLI-D-21-0193.1)

644 Yan H, Zhu Z, Wang B, Zhang K, Luo J, Qian Y and Jiang Y 2021 Tropical African wildfire aerosols
 645 trigger teleconnections over mid-to-high latitudes of Northern Hemisphere in January
 646 *Environmental Research Letters* **16** 034025

647 Yu, P., Toon, O. B., Bardeen, C. G., Zhu, Y., Rosenlof, K. H., Portmann, R. W., Thornberry, T. D.,
 648 Gao, R., S., Davis, S. M., Wolf, E. T., Gouw, J. d., Peterson, D. A., Fromm, M. D., and
 649 Robock, A.: 2019 Black carbon lofts wildfire smoke high into the stratosphere to form a
 650 persistent plume, **365**, 587-590, doi:10.1126/science.aax1748, 2019-90

651 Yue, X. and Unger, N.: Yue X, Strada S, Unger N and Wang A 2017 Future inhibition of ecosystem
 652 productivity by increasing wildfire pollution over boreal North America *Atmos. Chem. Phys.* **17**
 653 13699-719

654 Yue X and Unger N 2015 The Yale Interactive terrestrial Biosphere model version 1.0: description,
 655 evaluation and implementation into NASA GISS ModelE2, *Geosci. Model Dev.*, **8**, 2399-2417,
 656 [10.5194/gmd-8-2399-2015](https://doi.org/10.5194/gmd-8-2399-2015), 2015-417

657 Yue, X. and Unger, N.: 2018 Fire air pollution reduces global terrestrial productivity, *Nature*
 658 *Communications*, **9**, 5413, [10.1038/s41467-018-07921-4](https://doi.org/10.1038/s41467-018-07921-4), 2018.

659 Yue, X., Strada, S., Unger, N., and Wang, A.: Future inhibition of ecosystem productivity by increasing
 660 wildfire pollution over boreal North America, *Atmos. Chem. Phys.*, **17**, 13699-13719, [10.5194/aep-17-](https://doi.org/10.5194/aep-17-13699-2017)
 661 [13699-2017](https://doi.org/10.5194/aep-17-13699-2017), 2017.

662 Zhuravleva, T. B., Kabanov, D. M., Nasrtdinov, I. M., Russkova, T. V., Sakerin, S. M., Smirnov, A.,
 663 and Holben, B. N.: 2017 Radiative characteristics of aerosol during extreme fire event over
 664 Siberia in summer 2012, *Atmos. Meas. Tech.*, **10**, 179-198, [10.5194/amt-10-179-2017](https://doi.org/10.5194/amt-10-179-2017), 2017-98

665 Zou, Y., Wang, Y., Qian, Y., Tian, H., Yang, J., and Alvarado, E.: 2020 Using CESM-RESFire to
 666 understand climate–fire–ecosystem interactions and the implications for decadal climate
 667 variability, *Atmos. Chem. Phys.*, **20**, 995-1020, [10.5194/aep-20-995-2020](https://doi.org/10.5194/aep-20-995-2020), 2020.

Formatted: Font: Bold

Formatted: Indent: Left: 0 cm, Hanging: 7.2 ch

Formatted: Font: Italic

Formatted: Font: Bold

Formatted: Indent: Left: 0 cm, Hanging: 7.2 ch

Formatted: Font: Bold

Formatted: Indent: Left: 0 cm, Hanging: 7.2 ch

Formatted: Font: Italic

Formatted: Font: Bold

Formatted: Font: Italic

Formatted: Font: Bold

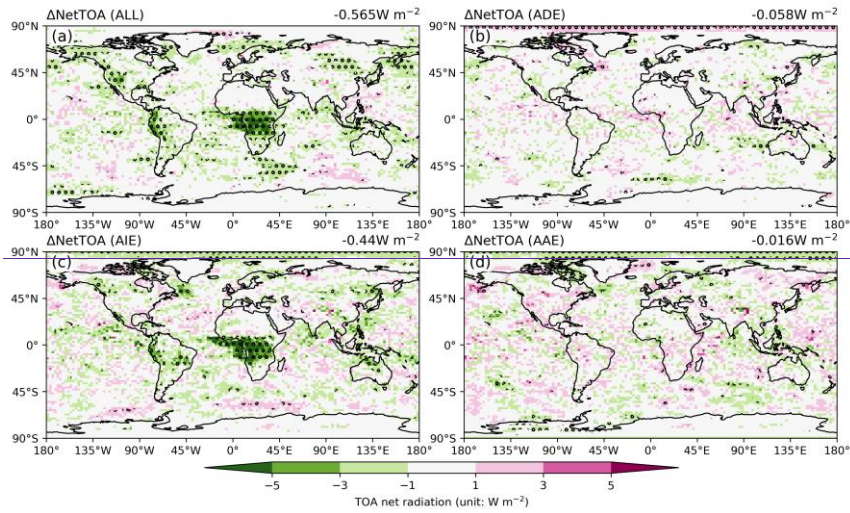
Formatted: Indent: Left: 0 cm, Hanging: 7.2 ch

Formatted: Font: Italic

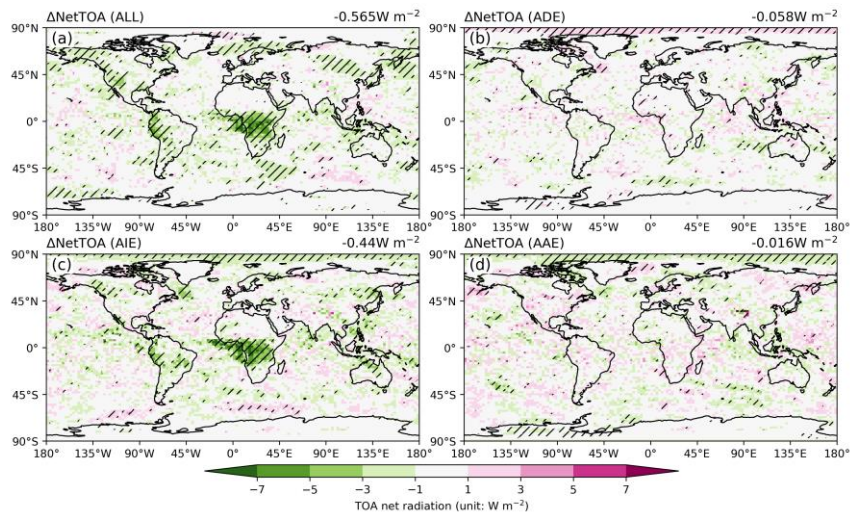
Formatted: Font: Bold

Formatted: Font: Italic

Formatted: Font: Bold



670

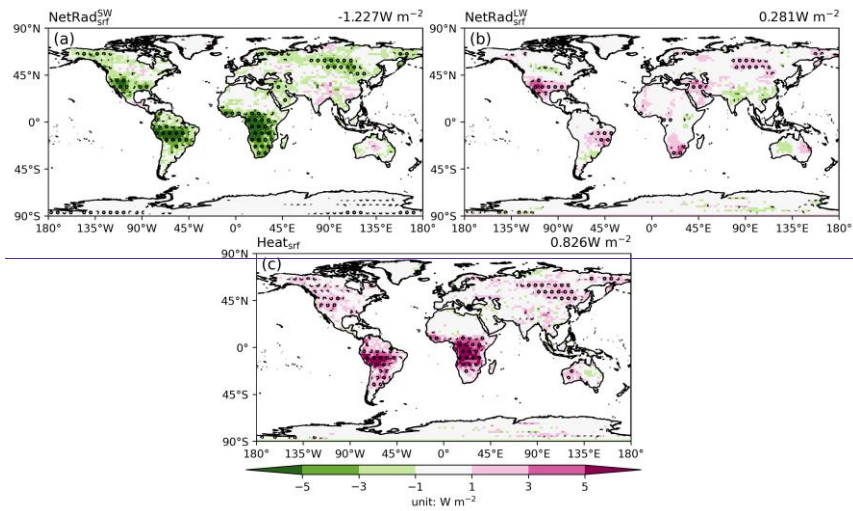


671

672 **Fig. 1** Changes in net radiation flux at top of atmosphere due to (a) total effects, (b) ADE, (c) AIE,
 673 and (d) AAE of fire aerosols. Positive values represent the increase of downward radiation. Global
 674 average is shown at the top of each panel. Dots denote areas with significant ($p < 0.1$) changes.
 675

Formatted: No widow/orphan control

Formatted: Font: Not Bold



676

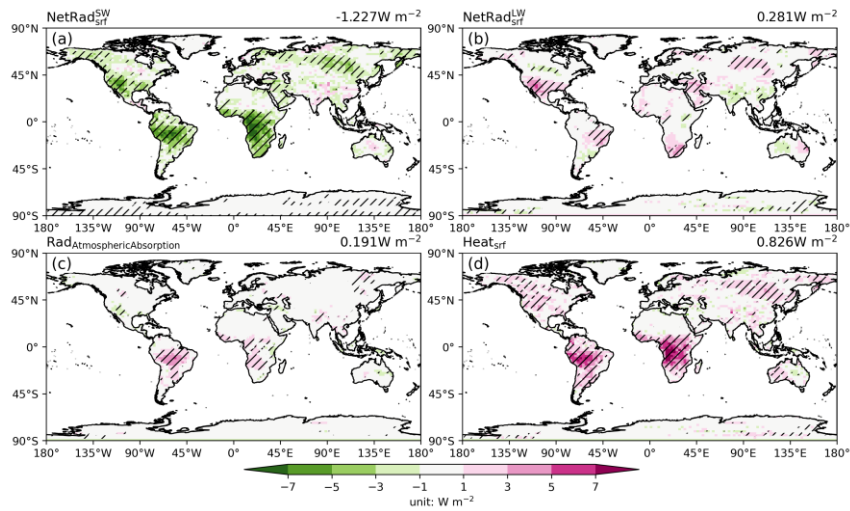
677 **Fig. 2** Changes in surface net (a) shortwave radiation, (b) longwave radiation, and (c) heat flux
 678 (sensible + latent) over land grids caused by fire aerosols. Positive values represent the increase of
 679 downward radiation. Global average value is shown at the top of each panel. Dots/Slashes denote
 680 areas with significant ($p < 0.1$) changes.

681

Formatted: Widow/Orphan control

Formatted

Formatted: Font: Bold



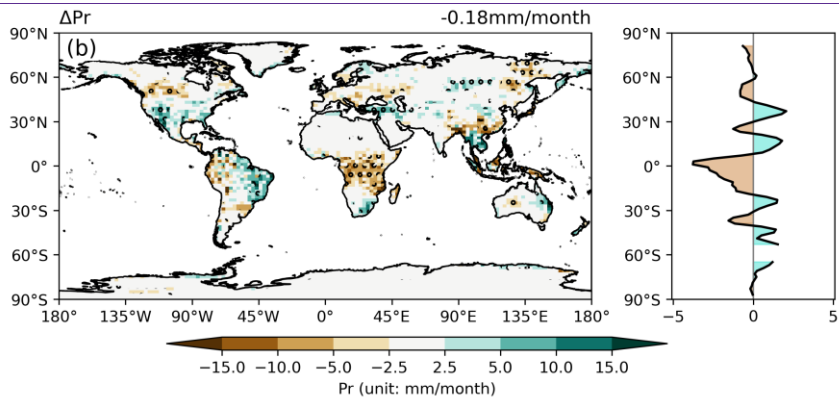
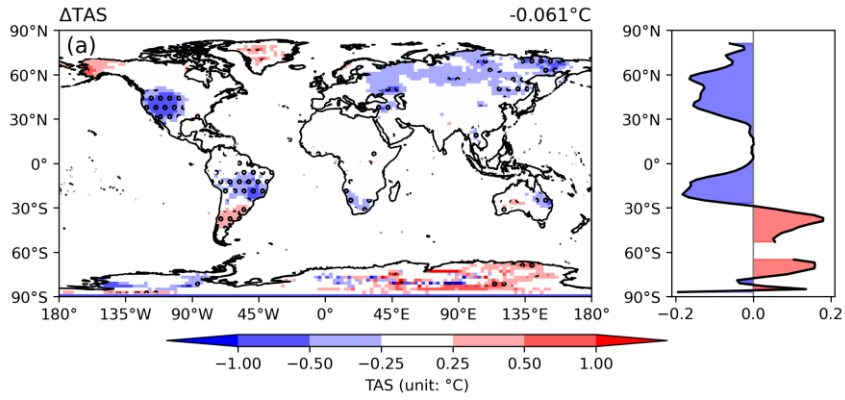
682

683 **Fig. 2** Changes in (a) surface net shortwave radiation, (b) surface net longwave radiation, (c)
 684 atmospheric absorbed radiation, and (d) surface heat flux (sensible + latent) over land grids caused
 685 by fire aerosols. Positive values represent the increase of downward radiation/heat for (a, b and d)
 686 and absorption for (c). Global land average value is shown at the top of each panel. Slashes denote
 687 areas with significant ($p < 0.1$) changes.

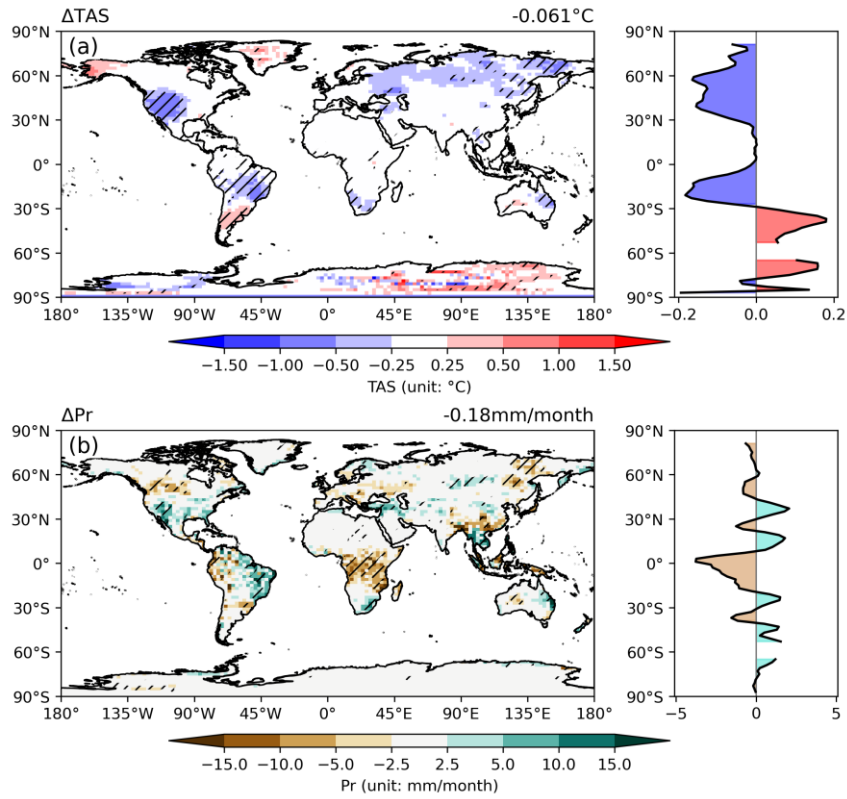
688

Formatted: No widow/orphan control

Formatted: Font: Not Bold

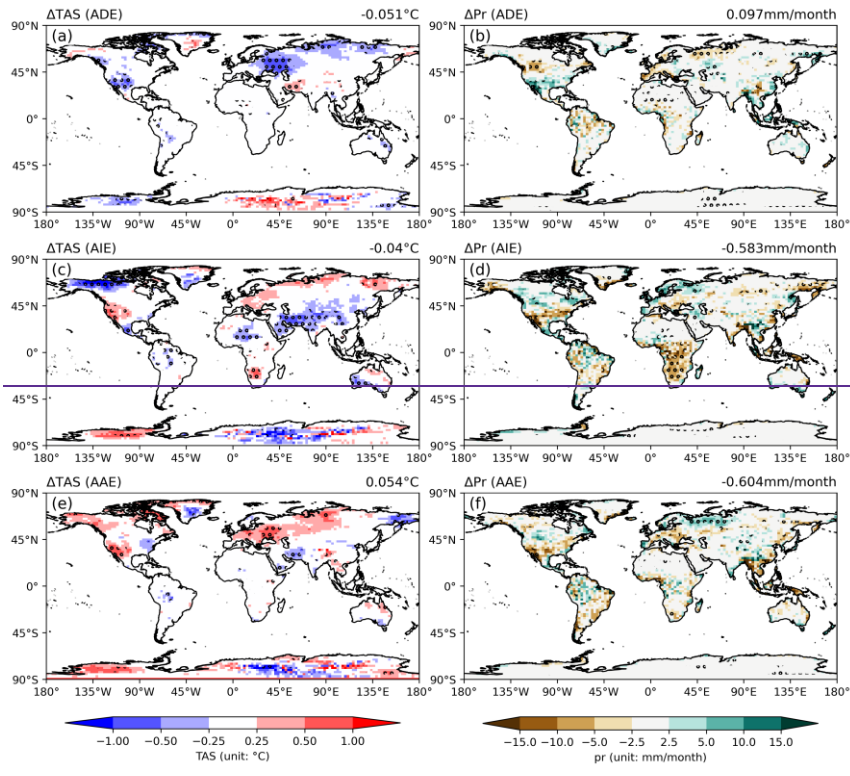


689

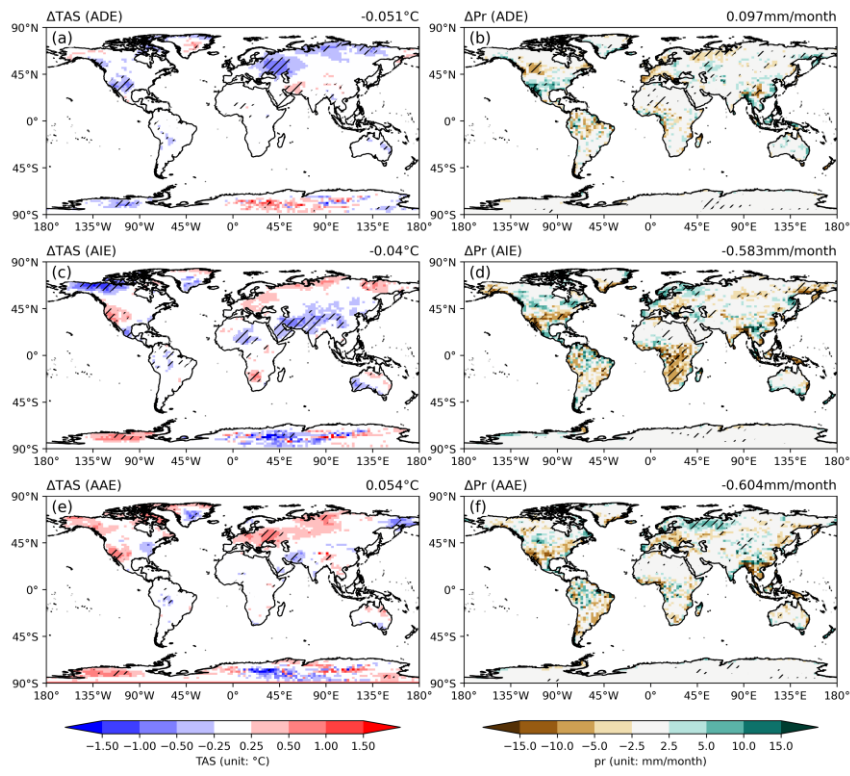


690

691 **Fig. 3** Changes in (a) surface air temperature and (b) precipitation over land grids caused by fire
 692 aerosols. The zonal averages of these changes are shown by the side of each panel. Global average
 693 value (land average for precipitation) value is shown at the top of each panel. Dots/Slashes
 694 denote areas with significant ($p < 0.1$) changes.
 695

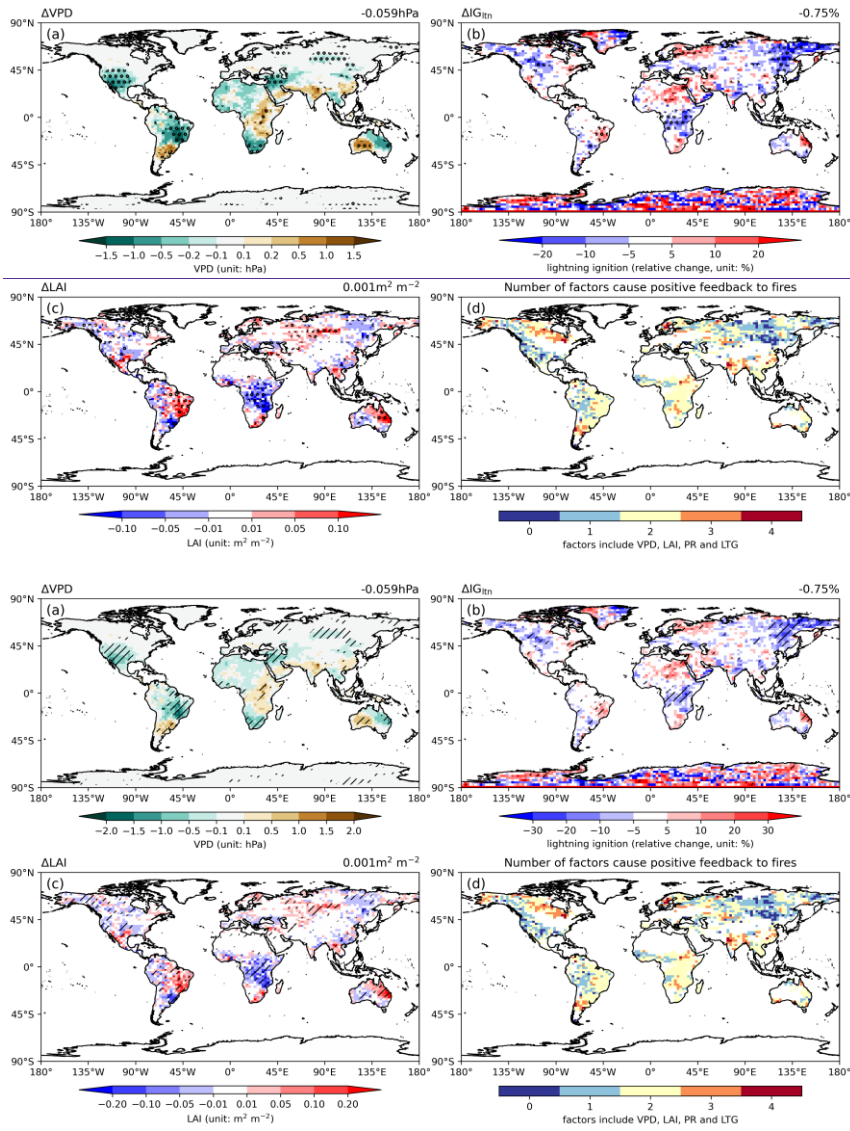


696



697

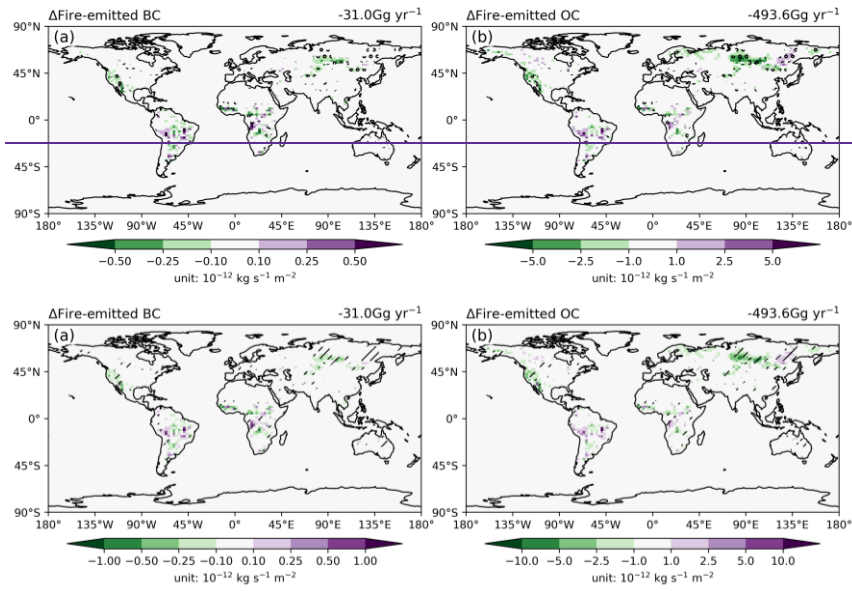
698 **Fig. 4** Changes in (a, c, e) surface air temperature and (b, d, f) precipitation over land grids due to
 699 (a, b) ADE, (c, d) AIE, and (e, f) AAE of fire aerosols. Global land average value is shown at the
 700 top of each panel. Dots/Slashes denote areas with significant ($p < 0.1$) changes.
 701



702

703

704 **Fig. 5** Changes in (a) vapor pressure deficit (VPD), (b) lightning ignition, and (c) leaf area index
 705 (LAI) over land grids induced by fire aerosols. Global land average value is shown at the top of
 706 each panel. ~~Dots/Slashes~~ denote areas with significant ($p < 0.1$) changes. The number of factors
 707 whose changes induced by fire aerosols cause positive feedback to fire emissions is shown in (d).
 708 Only grids with fire-emitted OC larger than $1 \times 10^{-12} \text{ kg s}^{-1} \text{ m}^{-2}$ (colored domain in Fig. S1b) are
 709 shown in (d).
 710



711

712

713 **Fig. 6** Changes in fire emissions of (a) BC and (b) OC through fire-climate interactions. The changes
 714 of fire emissions are calculated as the differences between YF_AD_AI_AA and NF_AD_AI_AA
 715 with dots/slashes indicating significant ($p < 0.1$) changes.
 716 The total emission is shown at the top of each panel.

Formatted: Justified

717

Table 1. Summary of simulations using ModelE2-YIBs

Simulation	Fires ^a	Aerosol direct effect	Aerosol indirect effect	Aerosol albedo effect
NF_AD	No	Yes	No	No
YF_AD	Yes	Yes	No	No
NF_AD_AI	No	Yes	Yes	No
YF_AD_AI	Yes	Yes	Yes	No
NF_AD_AA	No	Yes	No	Yes
YF_AD_AA	Yes	Yes	No	Yes
NF_AD_AI_AA	No	Yes	Yes	Yes
YF_AD_AI_AA	Yes	Yes	Yes	Yes

718

719 ^a All simulations predict fire emissions but the runs with NF do not feed the fire aerosols into the
 720 model to perturb radiative fluxes.

721

722
723

Table 2. Comparison of the simulated fire-induced change in radiative forcings at TOA and surface climate with previous studies

Reference	RF (W m ⁻²)	ADE (W m ⁻²)	AIE (W m ⁻²)	AAE (W m ⁻²)	TAS (°C)	Pr (mm month ⁻¹)
Ward et al. (2012)^a Ward et al. (2012)^a	-0.55	0.10	-1.00	0.00	—	—
Heald et al. (2014) Heald et al. (2014)	—	-0.19	—	—	—	—
Veira et al. (2015) Veira et al. (2015)	—	-0.20	—	—	—	—
Grandey et al. (2016) Grandey et al. (2016)	-1.0	0.04	-1.11	-0.1	—	-0.018
Jiang et al. (2016) Jiang et al. (2016)	-0.51	0.16	-0.70	0.03	-0.03	-0.3
Zou et al. (2020) Zou et al. (2020)	-0.59	-0.003	-0.82	0.19	—	—
Xu et al. (2021) Xu et al. (2021)	-0.73	0.25	-0.98	—	-0.17	-1.2
Yan et al. (2021) Yan et al. (2021)	<u>-0.62</u>	<u>0.17</u>	<u>-0.74</u>	<u>-0.04</u>	<u>0.03</u>	<u>—</u>
This study	-0.565	-0.058	-0.440	-0.016	-0.061	-0.18180

724
725

^a other effects of fire-induced on radiative turbulances are considered in this paper

Formatted Table

Formatted Table